Pharm Res (2012) 29:362–374
DOI 10.1007/s11095-011-0554-y

RESEARCH PAPER

Cationic Lipid-Coated Gold Nanoparticles as Efficient and Non-Cytotoxic Intracellular siRNA Delivery Vehicles

Won Ho Kong • Ki Hyun Bae • Sung Duk Jo • Jee Seon Kim • Tae Gwan Park

Received: 16 May 2011 / Accepted: 1 August 2011 / Published online: 13 August 2011

ABSTRACT

Purpose Cationic lipid-coated gold nanoparticles were developed for efficient intracellular delivery of therapeutic siRNA.

Methods Particle formation was characterized by UV-visible spectroscopy, atomic force microscopy, and dynamic light scattering analysis. Cellular uptake, gene silencing effect, and cytotoxicity were investigated in multiple human cancer cell lines.

Results Nanoparticles had a spherical nanostructure with highly cationic surface charge and could form stable nanosized polyelectrolyte complexes with siRNA via electrostatic interactions; complexes exhibited efficient intracellular uptake and significant gene silencing effect with markedly low cytotoxicity compared to the widely used polycationic carrier, linear polyethyleneimine.

Conclusions We demonstrated that cationic lipid-coated gold nanoparticles could be widely utilized as efficient and safe siRNA nanocarriers for diverse therapeutic and diagnostic applications.

Won Ho Kong and Ki Hyun Bae contributed equally to this work as first authors. The authors express their sincere condolences to family on the death (April 10, 2011) of Prof. Tae Gwan Park.

Electronic Supplementary Material The online version of this article (doi:10.1007/s11095-011-0554-y) contains supplementary material, which is available to authorized users.

W. H. Kong • K. H. Bae • S. D. Jo • J. S. Kim • T. G. Park
Department of Biological Sciences
Graduate School of Nanoscience & Technology
Korea Advanced Institute of Science & Technology
Daejeon 305-701, South Korea

W. H. Kong (✉)
Department of Material Science & Engineering
Pohang University of Science & Technology
San 31, Hyoja-dong, Nam-gu
Pohang 790-784, South Korea
e-mail: whkong@postech.ac.kr

KEY WORDS cancer therapy · cationic lipid · delivery system · gold nanoparticle · siRNA

INTRODUCTION

Over the past few decades, gold nanoparticles (AuNPs) have received a lot of attention in a broad range of biomedical fields, including biomolecular sensing, drug delivery, photothermal cancer therapy, and X-ray computed tomography (CT) imaging (1,2). Particularly in drug delivery, AuNPs have emerged as an attractive candidate for the creation of efficient nucleic acid delivery systems, mostly due to their excellent biocompatibility, versatility in synthesis, high surface-area-to-volume ratio, and facile surface functionalization through intracellularly displaceable gold-thiol linkages (1,2). Until recently, various types of AuNPs have been widely explored for intracellular delivery of nucleic acid drugs, such as plasmid DNA, antisense oligonucleotide, and small interfering RNA (siRNA) (2–10). Furthermore, AuNPs functionalized with bio-recognizable ligands have been developed for specific cell-targeting and delivery applications (11,12).

RNA interference (RNAi), which is an evolutionally conserved defense mechanism, holds great potential to treat various human diseases by silencing disease-causing genes using siRNA triggers (13). Although a wide variety of viral and non-viral siRNA delivery vehicles have been actively explored, there are still several challenges confronting the realization of RNAi therapeutics (14–18). For example, the practical application of siRNA is severely limited by its poor cellular uptake efficiency, failure of endosomal escape, and rapid enzymatic degradation in the bloodstream (14–18). During the last decade, a great effort has been directed

toward the development of cationic lipid-based siRNA nanocarriers, including emulsions, micelles, liposomes, and solid lipid nanoparticles (SLNs) (19–21). Among them, SLNs have attracted much attention as a promising alternative to the traditional siRNA vehicles (nanoemulsions, micelles, and liposomes) because of their high transfection efficiency, enhanced pharmacokinetic properties, and relatively low cytotoxicity (22). We have recently developed a new class of cationic SLNs whose compositions were reconstituted from those of natural apolipoprotein-free low-density lipoproteins (LDL). These cationic SLNs could deliver siRNA into cancer cells efficiently and thus displayed excellent gene inhibition effect while eliciting extremely low cytotoxicity (23).

When designing SLNs for drug delivery applications, the stable assembly of the lipid building blocks is of the utmost importance. For this purpose, the type and ratio of each lipid component and manufacturing procedures should be carefully optimized (21). However, the optimization processes are highly time-consuming and hard to achieve. In addition, the particle size and surface charge of SLNs needs to be suitably engineered to achieve specific targetability for their desirable functions in the body. For instance, recent studies have shown that the lipid nanoparticles for hepatocyte-targeted gene delivery must be smaller than 100 nm because the liver sinusoidal fenestrae are usually 100 nm in diameter (24–26). Likewise, the surface charge of SLNs is known to play an important role in acquiring improved colloidal stability in physiological environments and biocompatibility upon intravenous administration (24–26). When the conventional top-down approach is used to fabricate the lipid nanoparticles, it is difficult to control the particle size and surface charge, often resulting in the production of non-uniform particles larger than 100 nm (24–26). To date, well-designed and controlled SLNs (sub-100 nm) have not yet been reported by using any one-step synthesis without the complicated optimization processes.

In this study, we developed cationic lipid-coated gold nanoparticles (L-AuNPs) for efficient intracellular delivery of therapeutic siRNA. Herein, we presented a simple bottom-up approach to the fabrication of L-AuNPs by using AuNPs as a scaffolding material to induce self-assembly of the lipid building blocks. Hydrophobic dodecanethiol-capped AuNPs with an average size of 5 nm were first prepared and then solubilized with three different lipid components in organic solvent. The subsequent emulsification and solvent evaporation process led to the swift assembly of the amphiphilic lipid building blocks around the AuNPs via hydrophobic interactions. The resultant L-AuNPs would possess a nanostructure composed of an outer cationic lipid shell surrounding an inner gold nanoparticle cluster core. L-AuNPs having a positively charged shell layer are expected to effectively condense siRNA molecules into stable nanosized polyelectrolyte complexes, thus allowing for efficient cellular internalization and gene silencing effect. The hydrodynamic size and morphology of L-AuNPs were confirmed dynamic light scattering (DLS) analysis and atomic force microscopy (AFM). We also investigated the cellular uptake, gene silencing efficacy, and cytotoxicity of L-AuNP/siRNA complexes to evaluate their potential applicability for cancer therapy and hepatitis B treatment.

MATERIALS AND METHODS

Materials

3β-[*N*-(*N*′,*N*′-dimethylaminoethane)-carbamoyl]-cholesterol (DC-Chol), L-α-dioleoyl phosphatidylethanolamine (DOPE), and cholesterol hydrochloride (Chol) were obtained from Avanti Polar Lipids (Alabaster, AL). Hydrogen tetrachloroaurate ($HAuCl_4$), triphenylphosphine (PPh3), borane-tert-butylamine complex, and 4',6-diamidino-2-phenylindole (DAPI) were purchased form Sigma-Aldrich (St. Louis, MO). Linear and branched polyethylenimine (M_w = 25 KDa), denoted as l-PEI and b-PEI, respectively, were purchased from Polysciences (Warrington, PA). GFP siRNA (siGFP; sense: 5′-AAC UUC AGG GUC AGC UUG CdTdT-3′ and antisense: 5′-GCA AGC UGA CCC UGA AGU UdTdT-3′), VEGF siRNA (siVEGF; sense: 5′-GGA GUA CCC UGA UGA GAU CdTdT-3′ and antisense: 5′-GAU CUC AUC AGG GUA CUC CdTdT-3′), GAPDH siRNA (siGAPDH; sense 5′-GUG UGA ACC AUG AGA AGU AdTdT-3′ and antisense 5′-UAC UUC UCA UGG UUC ACA CdTdT-3′), HBV siRNA (siHBV; sense strand 5′-AAG AGG ACU CUU GGA CUC UCU U-3′ and antisense 5′-GAG AGU CCA AGA GUC CUC UUU U-3′) and siRNAs containing a fluorescent TAMRA and FAM-labeled sense strand were provided by Bioneer Co. (Daejeon, Korea). Ubiquitin B siRNA (siUBB) was kindly donated by Genolution Pharmaceuticals, Inc. (Seoul, Korea). Quantikine human VEGF immunoassay kit (R&D System, Minneapolis, MN) and EZ-Cytox Cell viability assay kit was (Daeil Lab Service, Seoul, Korea) were used according to the manufacturer's instructions. All other chemicals were of analytical reagent grade.

Synthesis of Cationic Lipid-Coated Gold Nanoparticle (L-AuNP)

For synthesis of L-AuNPs, dodecanethiol-capped gold nanoparticles (AuNPs) were first produced by the method described previously (27,28). In brief, a gold-triphenylphosphine complex (Au(PPh3)Cl) was synthesized by reacting $HAuCl_4$

solution (1.0 mg, 25.4 mmol) with PPh3 (1.4 mg, 5.2 mmol) in 35 mL of degassed 95% ethanol solution. The formed Au(PPh3)Cl (247 mg) was mixed with 250 μL of dodecanethiol in 40 mL of benzene. Borane-tert-butylamine complex (435 mg) was then added to the mixture and stirred for 1 h at 55°C to induce the reduction of gold precursor anions. The resulting product was retrieved as a dark red solid by centrifugation at 600×g and then purified by repetitive cycles of dispersion in ethanol and centrifugation. After residual ethanol was removed under reduced pressure, AuNPs were re-dispersed in chloroform at a concentration of 30 mg/mL. L-AuNPs were prepared by a modified emulsification/solvent evaporation method (27,28). Briefly, DC-Chol (16.1 mg, 54% *w*/*w*), DOPE (8.1 mg, 27% *w*/*w*), and Chol (5.8 mg, 19% *w*/*w*) were co-dissolved in 1.5 mL of chloroform/methanol mixture (2:1, *v*/*v*) containing AuNPs (15 mg). After 10 mL of deionized water was added, the mixture was vortexed for 2 min and subsequently sonicated for 3 min using a Bronson Sonifier 450 equipped with a micro-tip (20 kHz, duty cycle = 35, output control = 3.5). The resulting suspension was transferred to a round-bottom flask, and then the solvent was rapidly evaporated at 35°C at 20 mmHg using a rotary evaporator (EYELA, Japan). The produced L-AuNPs were purified by extensive dialysis against deionized water (M_w cut-off of 100 kDa).

Nanoparticle Characterization

The core size and shape of AuNPs were examined by transmission electron microscopy (TEM). For TEM observation, 30 μL of colloidal AuNP suspension was air-dried on a 300-mesh Formvar/carbon-coated copper grid and then observed by a Philips TECNAI F20 field emission TEM (Eindhoven, The Netherlands). Topological analysis of L-AuNPs and L-AuNP/siRNA complexes was carried out by tapping mode atomic force microscopy (AFM). For AFM observation, 50 μL of the sample solution was deposited onto a clean mica surface, and the images were then obtained using a Veeco NanoScope IV Multimode AFM (Santa Barbara, CA). The average particle size was determined by measuring the diameters of more than 50 particles in the images. UV-visible spectra were measured on a Shimadzu UV1601 spectrophotometer. The hydrodynamic diameter and zeta potential value of L-AuNPs and L-AuNP/siRNA complexes were measured in 0.1 M phosphate-buffered saline (PBS, pH 7.4) solution at 37°C using a Zetasizer Nano ZS (Malvern, UK). Each sample was properly diluted to maintain a count rate of around 200 and measured at least in triplicate.

Polyelectrolyte Complex Formation and Heparin-Displacement Assay

For the preparation of polyelectrolyte complexes, L-AuNPs were gently mixed with siRNA at various weight ratios of L-AuNP to siRNA in 0.1 M PBS solution (pH 7.4) and then incubated for 5 min at room temperature. The resultant complexes were characterized by agarose gel electrophoresis for 10 min at 100 V in TAE buffer solution (40 mM Tris-HCl, 1% (*v*/*v*) acetic acid, and 1 mM EDTA). After staining with ethidium bromide, the gel image was taken under UV illumination. To demonstrate the formation of electrostatic complexes between L-AuNP and siRNA, heparin displacement assay was performed. The polyelectrolyte complexes were formulated with 1 μg of siRNA at the weight ratio of 28 and then treated with heparin sodium salt solution at varying concentrations (0, 30, 60, and 90 μg/mL) for 15 min. The released siRNA was analyzed by agarose gel electrophoresis.

Evaluation of Gene Silencing Effect of L-AuNP/siRNA Polyelectrolyte Complexes

Cell Culture

GFP overexpressing MDA-MB-435 (human melanoma) and A549 (human lung carcinoma) cell lines were provided from Samyang Corp. (Daejeon, Korea). PC-3 (human prostate carcinoma) and HepG2 (human hepatoma) cell lines were acquired from the Korea Cell Line Bank (Seoul, Korea). HepG2.2.15 (Hepatitis B virus (HBV)-producing hepatoma) cell line was kindly donated by professor YH, Kim (Suwon Univ., Korea) and cultured in MEM medium (GIBCO, Glasgow, UK) supplemented with 10% (*v*/*v*) fetal bovine serum (FBS) and G418 antibiotic solution (200 μg/mL). The other cell lines were cultured in RPMI-1640 medium supplemented with 10% (*v*/*v*) FBS, 100 units/mL penicillin, and 100 μg/mL streptomycin.

GFP Gene Silencing Experiments

GFP overexpressing MDA-MB-435 and A549 cells were inoculated in a 24-well plate at a density of 2×10^5 cells per well and incubated for 24 h at 37°C. The cells were then incubated with L-AuNP/siGFP polyelectrolyte complexes at concentrations up to 71.4 nM (1 μg/mL) in the culture medium with or without FBS. After 5 h post-treatment, the cells were supplied with fresh FBS-supplemented medium and further cultivated for 48 h. As a control experiment, the cells were also treated with l-PEI/siGFP complexes (71.4 nM of siGFP) prepared at the nitrogen/phosphate (N/P) ratio of 20. The treated cells were washed with PBS solution and lysed with 0.1% Triton X-100 solution. After

centrifugation at 10,000 rpm for 5 min, the GFP concentration in the supernatant was analyzed using a LSM-AMINCO 8100 fluorophotometer (LSM, Urbana, IL) with an excitation wavelength at 488 nm and an emission wavelength at 509 nm. The relative GFP expression level was calculated based on the GFP expression of untreated cells, which was set to 100%.

VEGF Gene Silencing Experiments

PC-3 cells were seeded in a 24-well plate at a density of 2×10^5 cells per well and cultivated for 24 h at 37°C. The cells were treated with L-AuNP/siVEGF complexes at concentrations up to 71.4 nM in the FBS-supplemented medium. As a control experiment, the cells were also treated with L-AuNP/siGAPDH complexes at the same concentrations. After 5 h post-treatment, the medium was replaced with a fresh culture medium and further cultivated for 6 h. Afterward, the medium was aspirated to remove endogenously secreted VEGF and then replaced with a fresh culture medium containing 20 μg/mL heparin. After 16 h of incubation, the concentration of VEGF released from the cells was measured by using a Quantikine human VEGF immunoassay kit. The treated cells were harvested, and total RNA was isolated by using the Trizol reagent (Invitrogen, Carlsbad, CA) according to the manufacturer's protocol. Semi-quantitative reverse transcriptase polymerase chain reaction (RT-PCR) was performed to measure the cellular VEGF mRNA level, according to our previous report (27,28). The relative band intensity was analyzed by agarose gel electrophoresis using Image J software (NIH Image).

UBB Gene Silencing Experiments

A549 cells were seeded in a 24-well plate at a density of 2×10^5 cells per well and cultivated for 24 h at 37°C. The cells were treated with L-AuNP/siUBB complexes at concentrations up to 40 nM in the FBS-supplemented medium. After 48 h post-treatment, the cytotoxicity was examined by using a EZ-Cytox Cell viability assay kit. Typically, 10 μL of EZ-Cytox reagent was added to 100 μL of serum-free medium in each well of the plate. After incubating the plate for 2 h at 37°C, the absorbance at 450 nm was measured using a Bio-Rad microplate reader. The relative cell viability was expressed as the percentage of viable cells with respect to the untreated control group.

Hepatitis B Virus Surface Antigen (HBsAg) Knockdown Experiments

HepG2.2.15 cells were inoculated in a 24-well plate at a density of 2×10^5 cells per well and cultivated for 24 h at 37°C. The cells were treated with L-AuNP/siHBV complexes at concentrations up to 200 nM in the FBS-supplemented medium. After 5 h of incubation, the culture medium was changed with a fresh culture medium and further cultivated for 6 h. The medium was aspirated to remove endogenously secreted HBsAg and then replaced with a fresh culture medium. After incubation for 24 h, the concentration of HBsAg released from the cells was measured by using a Genedia HBsAg ELISA 3.0 kit (Green Cross, Korea).

Confocal Microscopy and FACS Analysis

Following the cultivation for 24 h on a cover slide at a density of 2×10^4 cells per slide, MDA-MB-435 and A549 cells were treated with L-AuNP/TAMRA-siRNA and L-AuNP/FAM-siRNA complexes (35.7 nM), respectively, for 3 h at 37°C. The cells were washed three times with PBS solution and then stained with DAPI (1.5 μg/mL in PBS solution) for 10 min. After fixation with 5% (*w*/*v*) formaldehyde solution, the cells were examined by using a LSM510 confocal laser-scanning microscope (Carl Zeiss, Germany). For FACS analysis, the MDA-MB-435 cells treated with L-AuNP/TAMRA-siRNA complexes were collected, washed with PBS solution three times, and then fixed by adding 5% (*w*/*v*) formaldehyde solution. As a control experiment, the cells were also treated with l-PEI/TAMRA-siRNA complexes at the N/P ratio of 20 and then harvested by the same procedures. The fluorescence of each cell was analyzed by a flow cytometer (FACSVantage, Franklin Lakes, NJ).

In Vitro Cytotoxicity Assay

MDA-MB-435 cells were seeded in a 48-well plate at a density of 2×10^4 cells per well and cultivated for 24 h at 37°C. The cells were incubated with L-AuNP, l-PEI, or b-PEI at varying concentrations up to 200 μg/mL for 10 h. The cytotoxicity was examined by using an EZ-Cytox Cell viability assay kit. In brief, the cells were washed with PBS solution and then treated with 10 μL of EZ-Cytox reagent for 2 h at 37°C. The relative cell viability was determined by measuring the absorbance at 450 nm using a Bio-Rad microplate reader and then normalized with respect to the untreated control group.

Micro-Computed Tomography (micro-CT) Imaging Procedure

Twenty-four hours prior to the treatment, MDA-MB-435 cells were seeded in a 100-mm culture dish at a density of 1×10^6 cells per dish. The cells were treated with L-AuNP/siRNA or l-PEI/siRNA complexes (71.4 nM) for 5 h at 37°C.

The cells were rinsed three times with PBS solution, harvested, and then centrifuged. The resulting cell pellets were mixed with 2% (*w*/*v*) low-melting agarose solution and transferred into a 1.5-mL Eppendorf tube. The embedded cells were visualized by using a micro-CT imaging device (Inveon Micro-CT, Siemens, USA).

RESULTS AND DISCUSSION

Design and Synthesis of Cationic Lipid-Coated Gold Nanoparticles

In this study, we fabricated cationic lipid-coated gold nanoparticles (L-AuNPs) for siRNA delivery applications. As illustrated in Fig. 1, hydrophobic dodecanethiol-capped gold nanoparticles (AuNPs) with an average size of 5 nm were first synthesized through the reduction of gold precursor anions in organic solvent (27,28). AuNP was selected as a scaffolding material for constructing an efficient siRNA nanocarrier due to their biocompatible and non-cytotoxic nature, high size controllability, and strong X-ray absorption ability desirable for computed tomography (CT) imaging (2–10). L-AuNPs were then prepared by a modified emulsification/solvent evaporation method. The hydrophobic AuNPs and three different lipid components were initially codissolved in a 2:1 chloroform: methanol solvent mixture. These lipid components were comprised of 3β-[*N*-(*N*′,*N*′-dimethylaminoethane)-carbamoyl]-cholesterol (DC-Chol, 54% *w*/*w*), L-α-dioleoyl phosphatidylethanolamine (DOPE, 27% *w*/*w*), and cholesterol (19% *w*/*w*). The compositions of the lipid building blocks were reconstituted from those of natural apolipoprotein-free low-density lipoproteins (LDL), as described in our previous report (23).

In the present study, the compositions were further optimized to create highly uniform and positively charged L-AuNPs. In this formulation, DC-Chol is a synthetic cholesterol analogue having a tertiary amine group and generates a cationic surface charge on L-AuNPs, allowing it to interact with anionic siRNA molecules to form polyelectrolyte complexes (21,23). DOPE has been utilized as a fusogenic helper lipid for improving gene transfection efficiencies of various liposomal formulations (21,23). Specifically, DOPE is known to enhance the intracellular uptake of polyelectrolyte complexes and to facilitate their endosomal escape by destabilizing the endosomal membranes via a pH-responsive phase transition. Cholesterol is a structural element in the cell membrane, which plays an important role in maintaining the membrane stability (21,23). It would not only increase the structural rigidity and stability of L-AuNPs, but also enhance the cellular permeability through the cell membranes via endocytosis-related cellular events (21,23,29). The solvent mixture containing the three lipid components and AuNPs was added dropwise to deionized water and ultrasonically treated to form a homogenous oil-in-water emulsion, where the hydrophobic AuNPs were localized inside oil phase droplets. The subsequent solvent evaporation procedure resulted in the swift assembly of the amphiphilic lipid building blocks around the AuNPs via hydrophobic interactions. After purification by excessive dialysis, L-AuNPs having an AuNP cluster core and a cationic lipid shell layer were successfully obtained.

Characterization of Cationic Lipid-Coated Gold Nanoparticles

The size distribution and surface morphology of gold nanoparticles were assessed by transmission electron microscopy (TEM) and atomic force microscopy (AFM). As shown in Fig. 2a, AuNPs were produced with a narrow size distribution of 5.1 ± 0.5 nm. In order to examine the formation of L-AuNPs, the optical properties of AuNPs and L-AuNPs were investigated by UV-visible spectroscopy. It has been shown previously

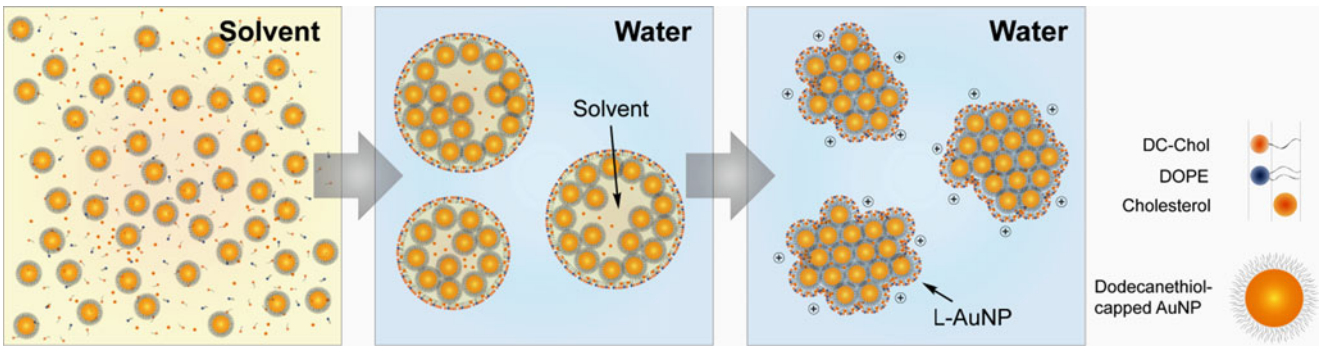

Fig. 1 Schematic illustration of the fabrication of cationic lipid-coated gold nanoparticles (L-AuNPs) via an emulsification/solvent evaporation process.

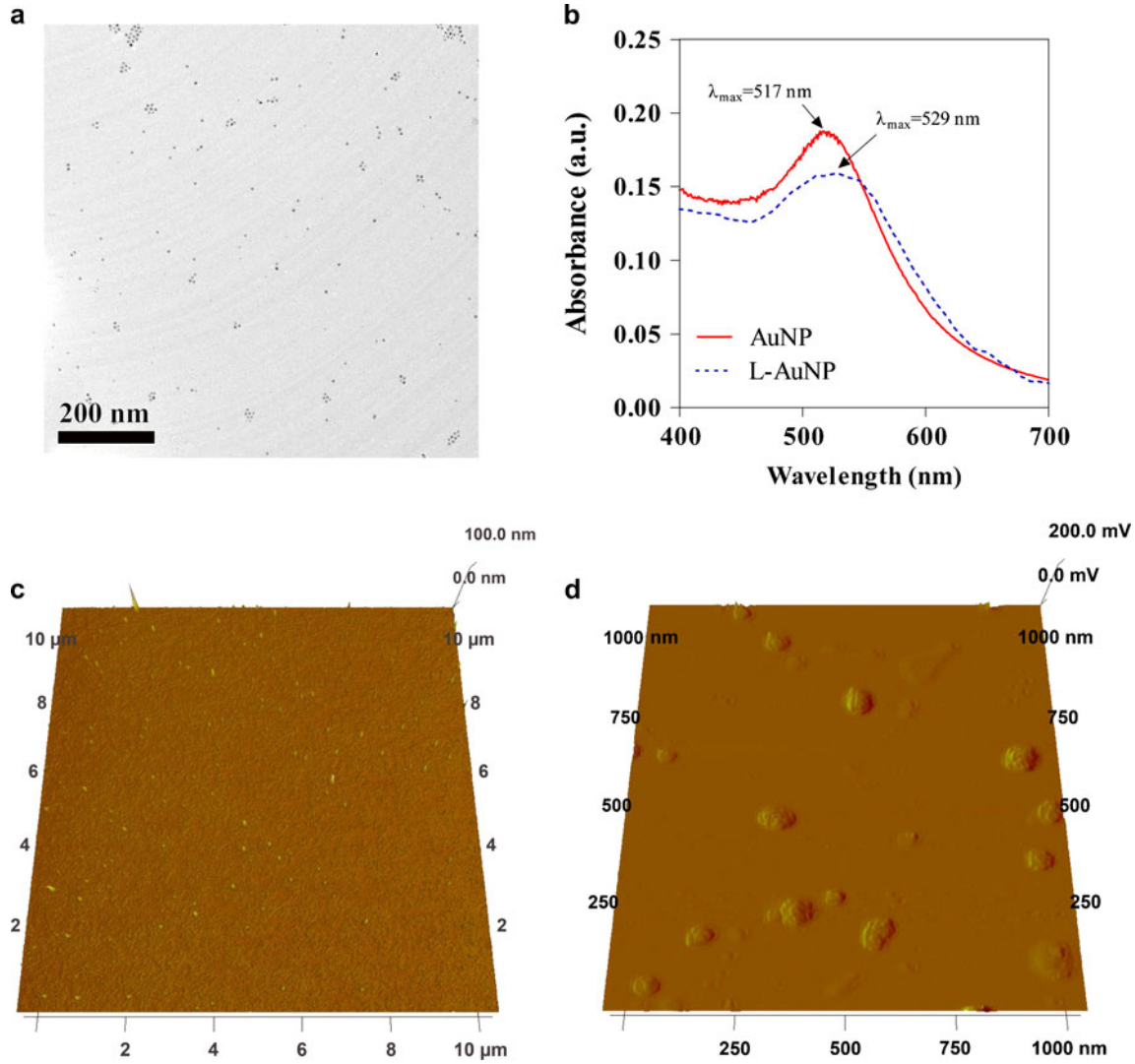

Fig. 2 (**a**) TEM image of dodecanethiol-capped gold nanoparticles (AuNPs). (**b**) UV-visible absorption spectra of AuNPs (*solid line*) and L-AuNPs (*dashed line*). (**c**) AFM height image and (**d**) amplitude image of L-AuNPs.

that the surface plasmon resonance (SPR) band of gold nanoparticles is influenced by their size, shape, aggregation state, and surrounding medium polarity (21,23,29). As presented in Fig. 2b, the SPR band of AuNPs appeared prominently at 517 nm, which was in agreement with the previous result (21,23,29). However, the UV-visible spectrum of L-AuNPs displayed a dramatic red shift of the SPR band up to 529 nm with peak broadening. This spectral change was likely attributed to the increased overlap of the surface plasmon between adjacent gold nanoparticles (21,23,29). Hence, it was conceivable that the distance between AuNPs decreased significantly when they were encapsulated within the outer lipid shell layer of L-AuNPs. As shown in the AFM height image (Fig. 2c), L-AuNPs had a well-dispersed and spherical nanostructure with an average diameter of 68.4±2.8 nm. Amplitude AFM analysis was also performed to visualize the spatial arrangement of gold nanoparticles of L-AuNPs. Since this technique detects the oscillation amplitude of the cantilever-tip at a fixed frequency, the AFM amplitude image displays the surface morphology of the sample more easily as compared to the height image (30). The AFM amplitude image (Fig. 2d) of L-AuNPs clearly showed that multiple gold nanoparticles were assembled into a larger three-dimensional cluster having a roughly spherical shape. Thus, the above results revealed that L-AuNPs possess a stable core-shell architecture composed of an outer cationic lipid shell layer encapsulating a gold nanoparticle cluster in the interior.

Formation of L-AuNP/siRNA Polyelectrolyte Complexes

To evaluate the applicability of the L-AuNPs as effective siRNA delivery vehicles, their siRNA binding ability was examined by agarose gel electrophoresis. When L-AuNPs were mixed with siRNA at various weight ratios ranging from 5 to 60 in 0.1 M PBS solution (pH 7.4), the electrophoretic migration of siRNA was completely retarded at the weight ratio of 25 (Fig. 3a). This result suggested that L-AuNPs having a cationic lipid shell layer effectively interacted with anionic siRNA molecules via electrostatic interactions (30). When preliminary gene silencing experiments were performed, maximum gene silencing effect was observed at the weight ratio of 28. Thus, L-AuNP/siRNA complexes prepared at this weight ratio were used for the rest of the study. As shown in Fig. 3b, the hydrodynamic diameter of L-AuNP/siRNA complexes (77.3±4.2 nm) was slightly larger than that of L-AuNPs (62.3±7.9 nm). In addition, the zeta potential value of L-AuNPs significantly decreased from 59.4±4.5 mV to 32.2±3.3 mV upon addition of siRNA (Fig. 3c), indicative of the reduction in the positive surface charge of L-AuNPs. These changes were probably ascribed to the association of siRNA molecules onto the surface of L-AuNPs. The AFM height image (Fig. 3d) showed that L-AuNP/siRNA complexes had a spherical shape and a similar size to that measured by the DLS analysis. It was also noteworthy that individual complexes were well dispersed without any severe aggregation, showing their excellent stability in aqueous solution. The AFM amplitude image revealed that the fluctuation amplitude of L-AuNP/siRNA complexes significantly increased as compared to L-AuNPs alone, indicating the formation of polyelectrolyte complexes larger than L-AuNPs (Supplementary Material, Fig. S1). To evaluate the formation of polyelectrolyte complexes between L-AuNP and siRNA, we conducted heparin-displacement assay. As shown in Fig. 3e, all siRNAs were completely released from L-AuNP/siRNA complexes after treatment with heparin sodium salt solution. Since this was a result of the dissociation of the complexes through competitive binding of negatively charged heparin molecules, it was evident that the electrostatic complex formation occurred between oppositely charged L-AuNP and siRNA. Therefore, these results demonstrated that L-AuNPs could form stable nanosized polyelectrolyte complexes capable of incorporating siRNA molecules and delivering them to desired cells or tissues.

Gene Silencing Effect of L-AuNP/siRNA Polyelectrolyte Complexes

To verify the capability of L-AuNP/siRNA polyelectrolyte complexes for efficient intracellular delivery of siRNA, their GFP gene silencing effect was examined in GFP over-expressing MDA-MB-435 and A549 cells at varying concentrations of siRNA. As presented in Fig. 4a, b (left panel), a significant dose-dependent inhibition of GFP expression was observed for both MDA-MB-435 and A549 cells treated with L-AuNP/siGFP complexes. It was worth noting that they exhibited far greater gene silencing effect than l-PEI/siGFP complexes. The L-AuNP/siGFP complexes significantly suppressed the GFP expression of MDA-MB-435 cells down to 47.7±1.0% at a concentration of 71.4 nM, whereas the l-PEI/siGFP complexes induced only slight gene inhibition to 82.5±2.3% under the same condition. The gene silencing efficiencies of the L-AuNP/siGFP complexes were also evaluated in the culture media containing 10% serum (Fig. 4a, 4b, right panel). The observed results were similar to those obtained under serum-deficient conditions, suggesting that the L-AuNP/siRNA complexes were able to inhibit the expression of target genes in cancer cells regardless of the presence or absence of serum. Serum stability studies using electrophoresis revealed that the L-AuNP/siRNA complexes effectively protected the incorporated siRNA molecules from degradation by serum nucleases (Supplementary Material, Fig. S2). Furthermore, these polyelectrolyte complexes maintained their structures without any sign of dissociation. Such excellent serum stability of the complexes was probably responsible for their efficient gene silencing effect in the presence of serum.

The therapeutic potential of L-AuNPs was investigated by evaluating the extent of VEGF down-regulation in cancer cells. VEGF is known to play an important role in regulating the process of tumor-induced angiogenesis essential for the survival, growth, and metastasis of solid tumors (31). Thus, there have been many attempts at developing non-viral carriers which can deliver anti-angiogenic siVEGF for cancer therapy (32,33). As shown in Fig. 4c (left panel), L-AuNP/siVEGF complexes gradually inhibited the release of VEGF from PC-3 cells in a dose-dependent manner, which was in accordance with the results observed for the L-AuNP/siGFP complexes. When the cellular VEGF mRNA level was evaluated by semi-quantitative RT-PCR, the relative band intensity decreased proportionally from 43.5±18.9% to 8.4±2.6% with increasing the siRNA concentration from 1.79 to 71.4 nM (Fig. 4c, right panel). From these results, it was conceivable that L-AuNP/siRNA complexes suppressed the target gene expression at both the protein and mRNA levels. Ubiquitin B (UBB) gene knockdown efficacy of L-AuNP/siUBB complexes was also evaluated in a similar manner (Fig. 4d). The ubiquitin-proteasome system is responsible for the degradation of intracellular proteins and a highly important process playing an essential regulatory role in cell survival and proliferation (34). Since the proteasome activity of UBB is selectively upregulated in tumor cells,

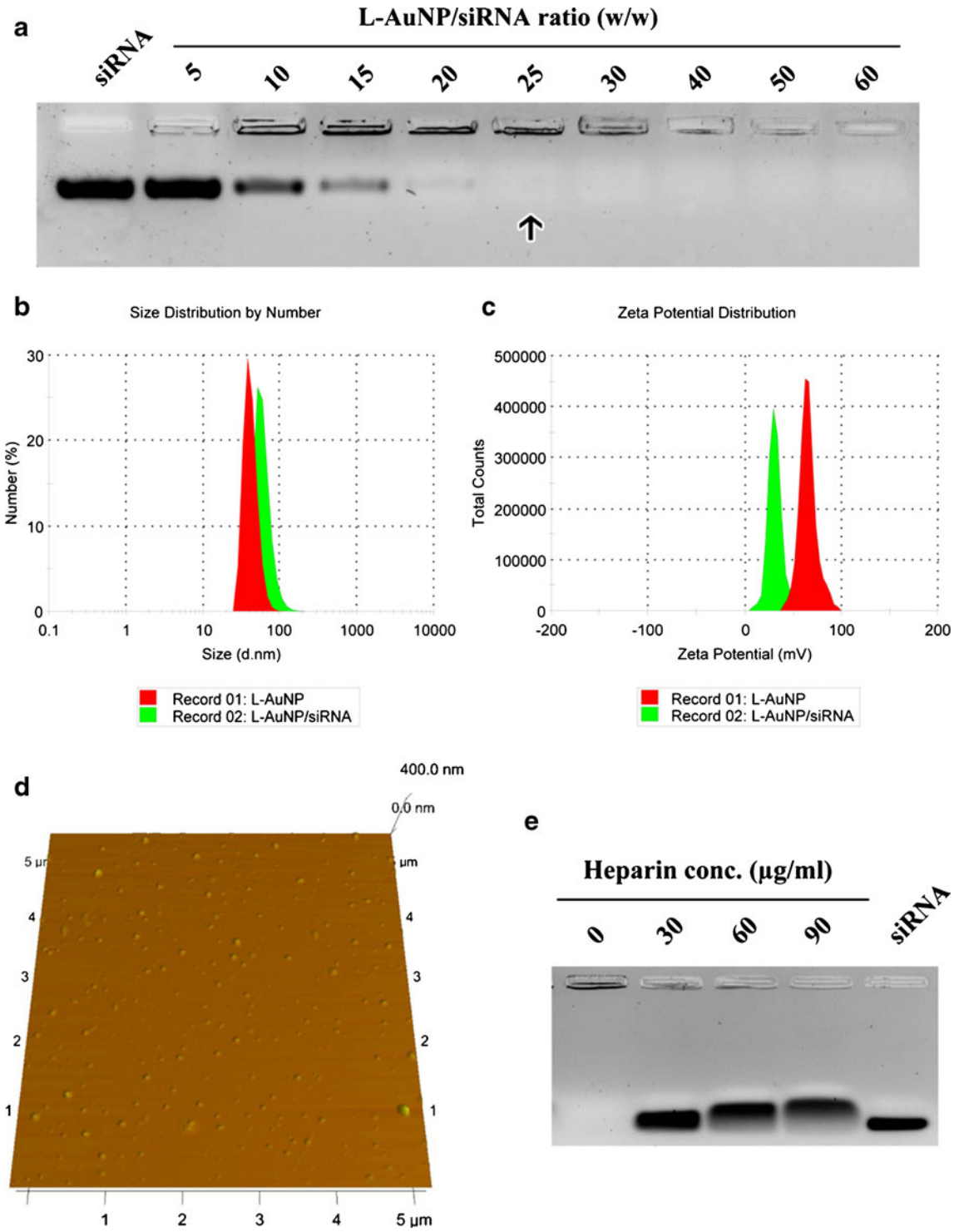

Fig. 3 (**a**) Agarose gel electrophoresis of L-AuNP/siRNA polyelectrolyte complexes prepared at various weight ratios of L-AuNPs to siRNA. The arrow indicates the weight ratio at which L-AuNPs completely inhibited the electrophoretic migration of siRNA. (**b**) Hydrodynamic diameters and (**c**) zeta potential values of L-AuNPs and L-AuNP/siRNA complexes prepared at the weight ratio of 28. (**d**) AFM height image of L-AuNP/siRNA complexes. (**e**) Heparin-displacement assay. Agarose gel electrophoresis of L-AuNP/siRNA complexes after treatment with heparin sodium salt solution at varying concentrations (0, 30, 60, and 90 μg/mL) for 15 min.

they are more sensitive to proteasome inhibitors than normal cells (34,35). Thus, the siRNA-mediated knockdown of UBB can be an effective strategy for cancer treatment. The L-AuNP/siUBB complexes showed the gradual decrease in the viability of A549 cells with increasing the concentrations up to 40 nM. This implies

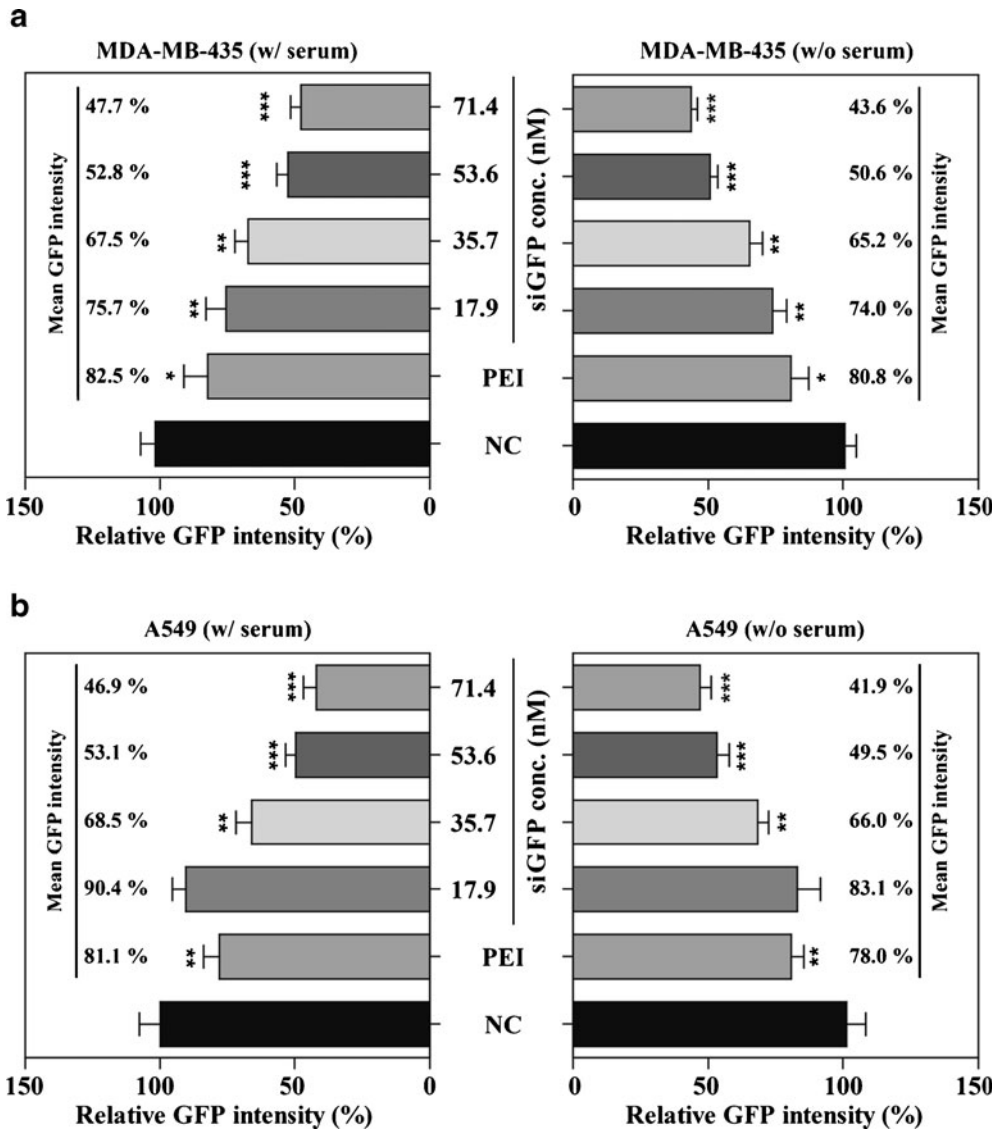

Fig. 4 Gene silencing effect of L-AuNP/siRNA complexes. Suppression of GFP gene expression in (**a**) MDA-MB 435 and (**b**) A549 cells treated with L-AuNP/siRNA or I-PEI/siGFP complexes at varying concentrations in the absence (*left panel*) and presence (*right panel*) of 10% serum. (**c**) Relative VEGF protein (*left panel*) and VEGF mRNA (*right panel*) level in PC-3 cells following incubation with L-AuNP/siVEGF complexes as a function of siVEGF concentration. The inset photographs display the RT-PCR band of VEGF and GAPDH mRNA transcripts on 1% agarose gel. (**d**) Viability of A549 cells treated with L-AuNP/siUBB complexes. (**e**) Relative HBsAg expression level of HepG2.2.15 cells after treatment with L-AuNP/siHBV complexes. Statistically significant difference from controls; * = $P < 0.05$, ** = $P < 0.01$, *** = $P < 0.001$.

that L-AuNP would be potentially utilized as a siRNA nanocarrier that can effectively suppress tumor growth by inducing the apoptotic death of cancer cells. To further validate the potential applicability of L-AuNPs for hepatitis B treatment, we examined the ability of L-AuNP/siHBV complexes to inhibit hepatitis viral replication in HBV-expressing HepG2.2.15 cells. To date, there is still a significant unmet medical need for safe and effective treatment of chronic HBV infection (36). Recent efforts have been devoted to developing a siRNA-based therapeutic strategy against chronic HBV infection (37,38). Particularly, siRNAs specific for three viral open reading frames (ORF) encoding the polymerase (P), surface (S), or X protein (X) have been shown to effectively inhibit the hepatitis viral expression and replication (37). In the current study, siHBV targeting an X ORF sequence was chosen to form polyelectrolyte complexes with L-AuNPs for inducing antiviral responses. As depicted in Fig. 4e, the release of hepatitis B virus surface antigen (HBsAg) was sharply reduced to 37.0±6.6% after treatment with 200 nM of the L-AuNP/siHBV complexes, indicating that they were able to block hepatitis viral replication efficiently. Taken together, the above results clearly revealed that the well-designed L-AuNP could deliver siRNA molecules into cancer cells and silence the target gene expression efficiently, thereby achieving excellent therapeutic effects.

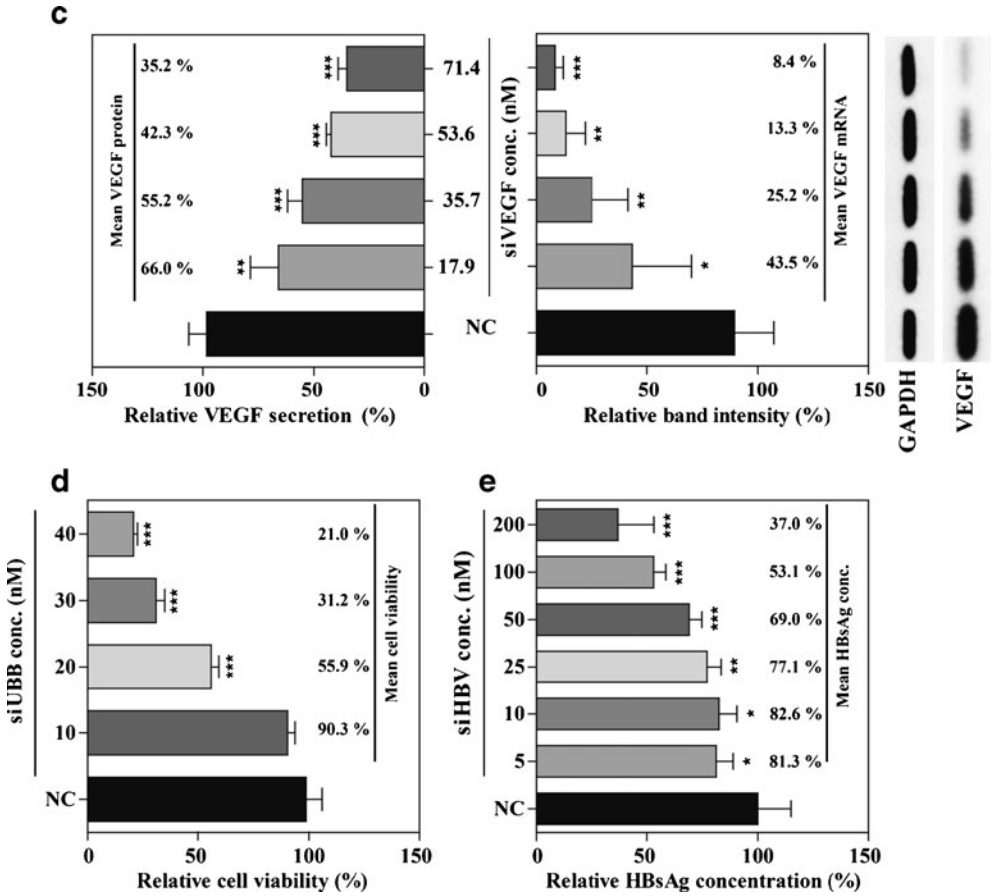

Fig. 4 (continued).

Cellular Internalization of L-AuNP/siRNA Complexes

For effective target gene silencing, it is crucial that siRNA should be efficiently taken up by cells and localized to the cytoplasm. Fluorescent FAM-siRNA or TAMRA-siRNA was associated to polyelectrolyte complexes, and their intracellular uptake was examined by confocal microscopy. As shown in Fig. 5a, b, a vast majority of fluorescently labeled complexes were internalized by the cells after 3 h of incubation. It was also found that the internalized complexes were evenly distributed inside the cells and finally diffused throughout the cytoplasm. The cellular uptake efficiency of L-AuNP/TAMRA-siRNA complexes was quantitatively evaluated by flow cytometric analysis (Fig. 5c). The extent of cellular uptake of these complexes was maximal; the percentage of TAMRA-positive cells reached about 96%. In contrast, only a moderate level of cellular uptake was observed for the l-PEI/siRNA complexes (Supplementary Material, Fig. S3). In addition, flow cytometry results showed more uniform cellular uptake of L-AuNP/siRNA complexes than l-PEI/siRNA complexes. This enhanced intracellular uptake of L-AuNP/siRNA complexes was likely responsible for their greater gene silencing effect compared to those of the l-PEI/siRNA complexes. Moreover, the fusogenic helper lipid components such as DOPE and cholesterol might facilitate the cellular entry and subsequent endosomal escape of the complexes, thus contributing to the observed efficient gene inhibition. Cellular internalization of the L-AuNP/siRNA complexes was further evidenced by micro-CT imaging. Gold nanoparticles have been widely explored as CT contrast agents because of their high electron density and strong X-ray absorption ability (39). As shown in the CT image (Supplementary Material, Fig. S4), the CT value for the cells treated with the complexes (16 HU) was much higher than that for the cells treated with the l-PEI/siRNA complexes (−7 HU). These results demonstrated that the L-AuNP/siRNA complexes exhibited remarkably greater cellular uptake compared to the l-PEI/siRNA complexes, as further supported by the micro-CT imaging analysis.

Cell Viability Studies

We also examined the cytotoxicity of L-AuNP, l-PEI, or b-PEI at various concentrations. As presented in

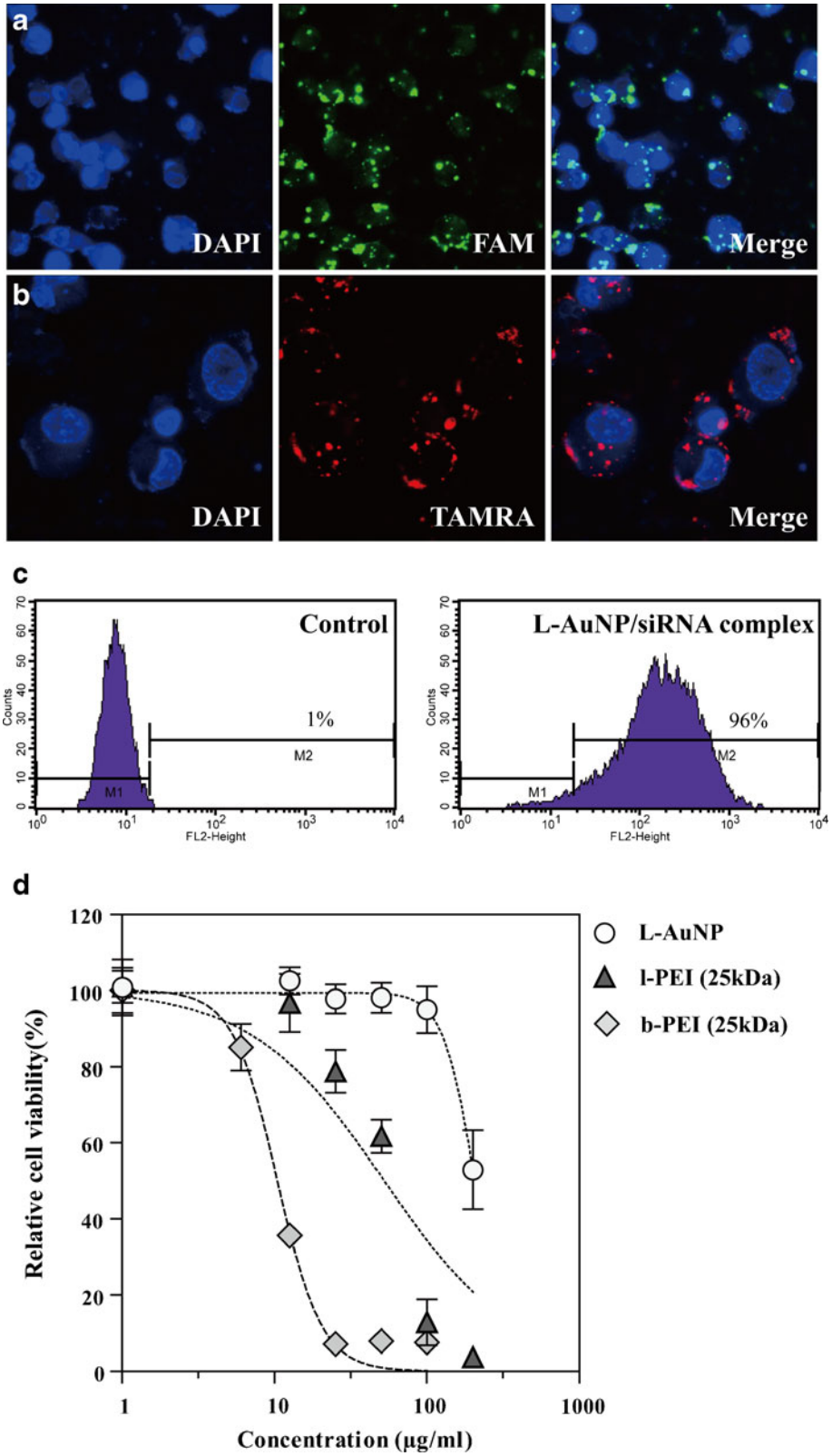

Fig. 5 Confocal microscopic images of (**a**) PC-3 and (**b**) MDA-MB-435 cells treated with L-AuNP/FAM-siRNA and L-AuNP/TAMRA-siRNA complexes, respectively. (**c**) Flow cytometry of MDA-MB-435 cells after incubation for 4 h with L-AuNP/TAMRA-siRNA complexes. (**d**) Cell viability following incubation with L-AuNP, l-PEI (25 kDa), and b-PEI (25 kDa) at different concentrations.

Fig. 5d, L-AuNP exhibited no severe cytotoxic effect up to a concentration of 100 μg/mL, whereas both l-PEI and b-PEI reduced the cell viability to around 5% at 100 μg/mL under the same conditions. The IC_{50} value of L-AuNP (206.7 μg/mL) was remarkably higher than those of b-PEI (10.4 μg/mL) and l-PEI (51.7 μg/mL).

From this result, it was evident that the significant gene silencing efficacy of L-AuNP/siRNA complexes was not attributed to the cytotoxic effect associated with the cationic L-AuNP vehicles. Consequently, the above results demonstrated that L-AuNPs could be widely utilized as efficient and safe nanovehicles for delivery of therapeutic siRNA to diseased cells or tissues. Furthermore, L-AuNPs having strong CT contrast ability were expected to be extensively applied for diverse diagnostic and therapeutic applications.

CONCLUSION

In summary, L-AuNPs having a cationic lipid shell layer were developed for efficient intracellular delivery of therapeutic siRNA. These nanoparticles were synthesized by a self-assembly of the lipid components reconstituted from natural LDLs. The produced L-AuNPs were able to form stable nanosized polyelectrolyte complexes with siRNA via electrostatic interactions. In addition, we demonstrated that L-AuNPs could efficiently deliver siRNA molecules into cancer cells, as well as significantly suppress the target gene expression without severe cytotoxicity as compared to linear PEI. These results suggested that L-AuNPs could be extensively utilized as efficient and non-cytotoxic intracellular siRNA delivery vehicles. Furthermore, the simple bottom-up approach described here provides a viable way to construct a wide variety of organic-inorganic hybrid nanomaterials for biomedical applications.

ACKNOWLEDGMENTS & DISCLOSURES

The late Professor Tae Gwan Park supervised the overall work as a principal investigator. All coauthors deeply appreciate his invaluable contribution and educational efforts. This research was supported by the Ministry for Health, Welfare and Family Affairs, and the World Class University project, Basic Science Research Program (2010–0027955) from the Ministry of Education, Science and Technology, Republic of Korea.

REFERENCES

1. Ghosh P, Han G, De M, Kim CK, Rotello VM. Gold nanoparticles in delivery applications. Adv Drug Deliv Rev. 2008;60:1307–15.
2. Guo S, Huang Y, Jiang Q, Sun Y, Deng L, Liang Z, *et al.* Enhanced gene delivery and siRNA silencing by gold nanoparticles coated with charge-reversal polyelectrolyte. ACS Nano. 2010;4:5505–11.
3. Lee JS, Green JJ, Love KT, Sunshine J, Langer R, Anderson DG. Gold, poly(beta-amino ester) nanoparticles for small interfering RNA delivery. Nano Lett. 2009;9:2402–6.
4. Giljohann DA, Seferos DS, Prigodich AE, Patel PC, Mirkin CA. Gene regulation with polyvalent siRNA-nanoparticle conjugates. J Am Chem Soc. 2009;131:2072–3.
5. Elbakry A, Zaky A, Liebl R, Rachel R, Goepferich A, Breunig M. Layer-by-layer assembled gold nanoparticles for siRNA delivery. Nano Lett. 2009;9:2059–64.
6. Rhim WK, Kim JS, Nam JM. Lipid-gold-nanoparticle hybrid-based gene delivery. Small. 2008;4:1651–5.
7. Li P, Li D, Zhang L, Li G, Wang E. Cationic lipid bilayer coated gold nanoparticles-mediated transfection of mammalian cells. Biomaterials. 2008;29:3617–24.
8. Y. Lee, S.H. Lee, J.S. Kim, A. Maruyama, X. Chen, and T.G. Park. Controlled synthesis of PEI-coated gold nanoparticles using reductive catechol chemistry for siRNA delivery. J Control Release (2010).
9. T. Niidome, K. Nakashima, H. Takahashi, and Y. Niidome. Preparation of primary amine-modified gold nanoparticles and their transfection ability into cultivated cells. Chem Commun (Camb):1978-1979 (2004).
10. Rosi NL, Giljohann DA, Thaxton CS, Lytton-Jean AK, Han MS, Mirkin CA. Oligonucleotide-modified gold nanoparticles for intracellular gene regulation. Science. 2006;312:1027–30.
11. Kubowicz S, Daillant J, Dubois M, Delsanti M, Verbavatz JM, Mohwald H. Mixed-monolayer-protected gold nanoparticles for emulsion stabilization. Langmuir. 2010;26:1642–8.
12. Cormode DP, Skajaa T, van Schooneveld MM, Koole R, Jarzyna P, Lobatto ME, *et al.* Nanocrystal core high-density lipoproteins: a multimodality contrast agent platform. Nano Lett. 2008;8:3715–23.
13. Mok H, Lee SH, Park JW, Park TG. Multimeric small interfering ribonucleic acid for highly efficient sequence-specific gene silencing. Nat Mater. 2010;9:272–8.
14. Higuchi Y, Kawakami S, Hashida M. Strategies for *in vivo* delivery of siRNAs: recent progress. BioDrugs. 2010;24:195–205.
15. Gilmore IR, Fox SP, Hollins AJ, Akhtar S. Delivery strategies for siRNA-mediated gene silencing. Curr Drug Deliv. 2006;3:147–5.
16. Park TG, Jeong JH, Kim SW. Current status of polymeric gene delivery systems. Adv Drug Deliv Rev. 2006;58:467–86.
17. Mokand H, Park TG. Functional polymers for targeted delivery of nucleic acid drugs. Macromol Biosci. 2009;9:731–43.
18. Ohand YK, Park TG. siRNA delivery systems for cancer treatment. Adv Drug Deliv Rev. 2009;61:850–62.
19. Mevel M, Kamaly N, Carmona S, Oliver MH, Jorgensen MR, Crowther C, *et al.* DODAG; a versatile new cationic lipid that mediates efficient delivery of pDNA and siRNA. J Control Release. 2010;143:222–32.
20. Semple SC, Akinc A, Chen J, Sandhu AP, Mui BL, Cho CK, *et al.* Rational design of cationic lipids for siRNA delivery. Nat Biotechnol. 2010;28:172–6.
21. Schroeder A, Levins CG, Cortez C, Langer R, Anderson DG. Lipid-based nanotherapeutics for siRNA delivery. J Intern Med. 2010;267:9–21.
22. Mukherjee S, Ray S, Thakur RS. Solid lipid nanoparticles: a modern formulation approach in drug delivery system. Indian J Pharm Sci. 2009;71:349–58.
23. Kim HR, Kim IK, Bae KH, Lee SH, Lee Y, Park TG. Cationic solid lipid nanoparticles reconstituted from low density lipoprotein components for delivery of siRNA. Mol Pharm. 2008;5:622–31.
24. Akinc A, Querbes W, De S, Qin J, Frank-Kamenetsky M, Jayaprakash KN, *et al.* Targeted delivery of RNAi therapeutics with endogenous and exogenous ligand-based mechanisms. Mol Ther. 2010;18:1357–64.
25. Kim SI, Shin D, Lee H, Ahn BY, Yoon Y, Kim M. Targeted delivery of siRNA against hepatitis C virus by apolipoprotein A-I-bound cationic liposomes. J Hepatol. 2009;50:479–88.

26. Tao W, Davide JP, Cai M, Zhang GJ, South VJ, Matter A, *et al.* Noninvasive imaging of lipid nanoparticle-mediated systemic delivery of small-interfering RNA to the liver. Mol Ther. 2010;18:1657–66.
27. Zheng N, Fan J, Stucky GD. One-step one-phase synthesis of monodisperse noble-metallic nanoparticles and their colloidal crystals. J Am Chem Soc. 2006;128:6550–1.
28. Brust M. Nanoparticle ensembles: nanocrystals come to order. Nat Mater. 2005;4:364–5.
29. Couto RD, Dallan LA, Lisboa LA, Mesquita CH, Vinagre CG, Maranhao RC. Deposition of free cholesterol in the blood vessels of patients with coronary artery disease: a possible novel mechanism for atherogenesis. Lipids. 2007;42:411–8.
30. Lauer ME, Grassmann O, Siam M, Tardio J, Jacob L, Page S, *et al.* Atomic force microscopy-based screening of drug-excipient miscibility and stability of solid dispersions. Pharm Res. 2011;28:572–84.
31. Ueda Y, Yamagishi T, Samata K, Ikeya H, Hirayama N, Takashima H, *et al.* A novel low molecular weight antagonist of vascular endothelial growth factor receptor binding: VGA1155. Mol Cancer Ther. 2003;2:1105–11.
32. Kim SH, Jeong JH, Lee SH, Kim SW, Park TG. Local and systemic delivery of VEGF siRNA using polyelectrolyte complex micelles for effective treatment of cancer. Journal of controlled release: official journal of the Controlled Release Society. 2008;129:107–16.
33. Kim SH, Jeong JH, Lee SH, Kim SW, Park TG. PEG conjugated VEGF siRNA for anti-angiogenic gene therapy. Journal of controlled release: official journal of the Controlled Release Society. 2006;116:123–9.
34. Wu P, Tian Y, Chen G, Wang B, Gui L, Xi L, *et al.* Ubiquitin B: an essential mediator of trichostatin A-induced tumor-selective killing in human cancer cells. Cell Death Differ. 2010;17:109–18.
35. Chenand D, Dou QP. The ubiquitin-proteasome system as a prospective molecular target for cancer treatment and prevention. Curr Protein Pept Sci. 2010;11:459–70.
36. M.F. Yuenand C.L. Lai. Treatment of chronic hepatitis B: Evolution over two decades. J Gastroenterol Hepatol. 26 Suppl 1:138-143 (2011).
37. Fu J, Tang ZM, Gao X, Zhao F, Zhong H, Wen MR, *et al.* Optimal design and validation of antiviral siRNA for targeting hepatitis B virus. Acta Pharmacol Sin. 2008;29:1522–8.
38. Chen Y, Cheng G, Mahato RI. RNAi for treating hepatitis B viral infection. Pharm Res. 2008;25:72–86.
39. Hainfeld JF, Slatkin DN, Focella TM, Smilowitz HM. Gold nanoparticles: a new X-ray contrast agent. Br J Radiol. 2006;79:248–53.